NOAA Technical Memorandum ERL WPL-163

REMOTE SENSING TECHNIQUES OF THE WAVE PROPAGATION LABORATORY FOR THE MEASUREMENT OF SUPERCOOLED LIQUID WATER: APPLICATIONS TO AIRCRAFT ICING

E. R. Westwater
R. A. Kropfli

Wave Propagation Laboratory
Boulder, Colorado
May 1989

noaa NATIONAL OCEANIC AND ATMOSPHERIC ADMINISTRATION / Environmental Research Laboratories

NOAA Technical Memorandum ERL WPL-163

REMOTE SENSING TECHNIQUES OF THE WAVE PROPAGATION LABORATORY FOR THE MEASUREMENT OF SUPERCOOLED LIQUID WATER: APPLICATIONS TO AIRCRAFT ICING

E. R. Westwater
R. A. Kropfli

Wave Propagation Laboratory
Boulder, Colorado
May 1989

UNITED STATES
DEPARTMENT OF COMMERCE

Robert A. Mosbacher
Secretary

NATIONAL OCEANIC AND
ATMOSPHERIC ADMINISTRATION

William E. Evans
Under Secretary for Oceans
and Atmosphere/Administrator

Environmental Research
Laboratories

Joseph O. Fletcher
Director

NOTICE

Mention of a commercial company or product does not constitute an endorsement by NOAA Environmental Research Laboratories. Use for publicity or advertising purposes of information from this publication concerning proprietary products or the tests of such products is not authorized.

For sale by the National Technical Information Service, 5285 Port Royal Road
Springfield, VA 22161

EXECUTIVE SUMMARY

The formation of ice on aircraft continues to be a significant hazard to lower atmospheric flight. For example, during the 5–1/2 year period beginning in January 1978, 280 icing-related accidents resulting in 364 fatalities were reported in the United States. Supercooled liquid water (SLW) along the flight path causes aircraft ice accumulation that results in such accidents. The amount of SLW needed to cause hazardous conditions is small; as little as 0.2 g/m^3 can result in significant ice accumulation if the flight path through the SLW region is sufficiently long. Not only is the amount of SLW important but the droplet size distribution also has a role; larger droplets impact more readily on aircraft surfaces. Because of their greater mass, droplets larger than about 30 μm are not deflected as much by the airflow across external surfaces, and they have a better opportunity than the smaller droplets to impact and freeze.

The microphysical processes and conditions that produce SLW in clouds are complicated and difficult to detect and to forecast. Temperature, droplet size distributions, amount of ice present, turbulence, vertical air motions, and vapor flux all interact to affect the formation of SLW. Furthermore, the presence of SLW (not directly observable either by conventional weather radars or by radiosondes) is usually known primarily through pilot reports. However, new remote sensing instruments and techniques developed recently at the NOAA/Wave Propagation Laboratory (WPL) can contribute to the solution because of their ability to detect SLW directly or to monitor parameters that eventually lead to the formation of SLW. Such systems could be useful in the operational sector by providing real-time guidance for aircraft operations and also by providing input data to icing forecast models. These remote sensing systems will also be of great value in icing research programs to help evaluate new forecasting techniques. It is feasible to vector instrumented research aircraft into regions suspected of having SLW.

Such remote sensing instruments available at WPL include the following:

(1) A transportable three-channel, steerable-beam, microwave radiometer and several fixed-site, two-channel, fixed-beam radiometers for integrated liquid and vapor measurements.

(2) A transportable Radio Acoustic Sounding System (RASS) for continuous monitoring of temperature profiles.

(3) Transportable Doppler radars for documentation of wind field anomalies that can provide lifting needed to create SLW.

(4) Dual-wavelength radar for spatial mapping of SLW.

(5) Transportable and fixed-site wind profiling radars for continuous wind monitoring.

These instruments, when used in combination as a *remote sensing system*, offer an array of new approaches for solving a difficult problem in which little progress has been made over the last several decades. This technical memorandum reviews the processes causing aircraft icing, describes promising new remote sensing instruments and methodologies, and suggests how these can be applied to help solve the aircraft icing problem.

CONTENTS

REMOTE SENSING TECHNIQUES OF THE WAVE PROPAGATION LABORATORY FOR THE MEASUREMENT OF SUPERCOOLED LIQUID WATER: APPLICATIONS TO AIRCRAFT ICING

E. R. Westwater and R. A. Kropfli

1. INTRODUCTION

For over twenty years, the Wave Propagation Laboratory (WPL) has developed a variety of remote sensing techniques applicable to cloud studies. We restrict our attention here to clouds with the potential to cause aircraft icing, i.e., clouds containing supercooled liquid water (SLW). We review existing and potential capabilities of modern ground-based remote sensors that are being developed and operated at WPL because such remote sensors can help with the solution of the aircraft icing problem. Although some WPL instruments have been components of cloud physics experiments for several years, new concepts, instruments, and combinations of instruments described here can make important contributions to both icing hazard research and to operations. We first identify important meteorological parameters, atmospheric mechanisms, and areas of need for the solution of the icing problem. We then show how these needs can be addressed by remote sensors.

2. METEOROLOGICAL FACTORS IN AIRCRAFT ICING: A SUMMARY OF NEEDS

2.1 Aircraft Icing: A Continuing Unsolved Problem

A significant number of accidents have resulted from ice accumulations on aircraft. Since general aviation and commuter flights spend a considerable fraction of total flight time in the lower troposphere, hazardous icing encounters are frequent. Recognition of the icing problem is not new. As noted by Riley (1937), "The formation of ice on aircraft is one of the greatest hazards to air traffic today, with the accompanying complications of turbulence which makes the airplane difficult to control..."

Almost 50 years later a remarkably similar statement was made by a review committee in the NASA Workshop on Meteorological and Environmental Inputs to Aviation Systems (Committee Report, 1985): "Currently there is a nearly complete lack of meaningful or adequate forecasts, or even nowcasts for icing conditions, particularly for commuter and general aviation." As an example of this, we note the summary of aircraft icing accidents for the period between January 1978 and June 1983 given by Czekalski (1985): During this period, 280 icing-related accidents occurred with 364 fatalities and 171 injuries. As we shall see, an understanding and definition of the morphology of supercooled liquid water will take us a long way toward the solution of this problem.

2.2 Microphysical Considerations

SLW droplets form in clouds when water vapor accumulates to saturation or supersaturation values and condenses on plentiful cloud condensation nuclei at temperatures below 0°C. Ice crystals are less readily and less abundantly nucleated in the atmosphere. Thus, at all but the coldest of tropospheric temperatures, clouds of SLW form first. Fogs of SLW may persist for hours as stable colloidal suspensions with no ice. Clouds driven primarily by atmospheric circulations or convection usually evolve more rapidly. In these clouds, the supercooled droplets may grow collectively by further condensation or selectively by collision coalescence as the concentrations of SLW increase and the droplet size spectrum broadens. Droplets as large as several hundred micrometers may form and precipitate. More often, the cloud circulations lead to further cooling and to the introduction of ice crystals that grow at the expense of the droplets, sometimes to sizes large enough to precipitate. The fluxes of liquid and ice that do not precipitate will return to the vapor phase upon exiting the cloud system or as the circulation wanes. The key here is that the *fluxes* of water substance at temperatures below 0°C control the formation of SLW. Figure 2.1 schematically indicates the different forcing mechanisms that can produce SLW.

It is important to measure the concentration of SLW *continuously*, to determine its presence in terms of integrated totals, or even better, its three-dimensional distribution, and its projected evolution. Warm-cloud liquid water ($T > 0°C$) must be distinguished from the SLW to evaluate aircraft icing hazards. Thus, the vertical profiles of atmospheric temperature and liquid water must be known, and the level of 0°C isotherm must be monitored. Drop size spectra need to be measured in both SLW and mixed-phase clouds so that we can completely understand the formation of SLW. Additionally, the drop size spectra and temperatures of freezing rain are another aspect of aircraft icing hazards. Hansman (1989) reviewed critical parameters that determine the formation of ice on aircraft surfaces, and we summarize his comments in Table 2.1.

Finally, we note that the *spatial distribution* of SLW influences the critical exposure time for an aircraft to experience icing. Improved forecasting and detection of the spatial distribution of SLW is needed to minimize aircraft residence time.

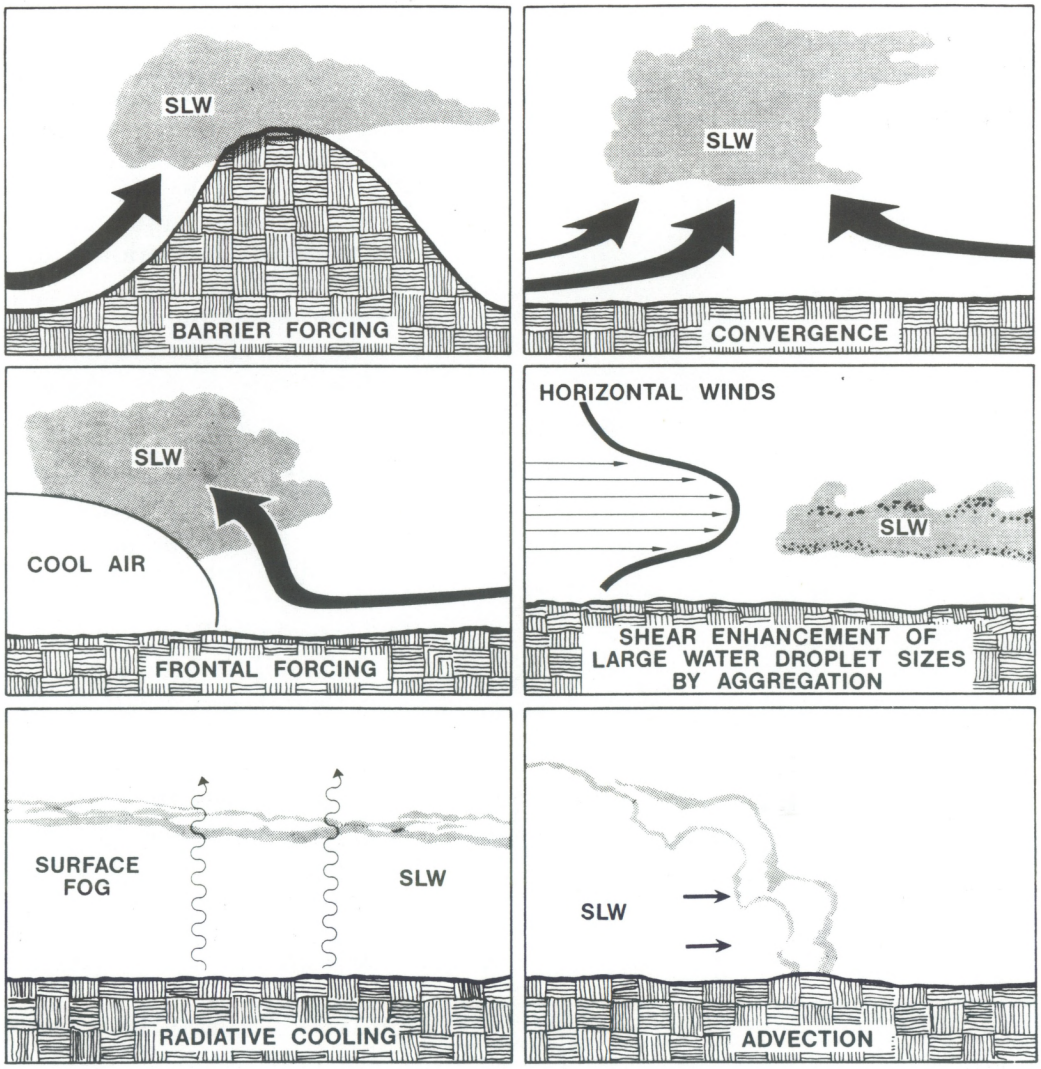

Fig. 2.1. Summary of atmospheric processes producing aircraft icing conditions.

Table 2.1. Summary of critical parameters that determine formation of ice on aircraft

Parameter	Comments
Liquid water content	Higher cloud SLW indicates greater severity. SLW content >0.1 g/m^3 is considered potentially hazardous.
Temperature	Hazardous conditions are most often found at temperatures between -10 and 0°C.
Droplet size distributions	Presence of large droplets can quickly produce ice loads. Clouds with appreciable concentrations of droplets with diameters between 30 and 400 μm are most hazardous.
Cloud phase mix (ice/liquid fraction)	The details of cloud phase can enhance or reduce aircraft icing potential and make prediction more difficult.
Turbulence	Can influence icing potential, but the dynamics are at present unclear.
Water vapor flux	Increased vertical flux of vapor will increase SLW content.
Cloud vertical motions	Large cloud droplets are most likely to develop where updrafts are intense and sustained.

2.3 A Summary of Research and Operational Needs

Figure 2.2 summarizes the research and operational needs for solution of the icing problem as expressed in Sections 2.1 and 2.2. The remainder of this report addresses how remote sensors can help fill these needs.

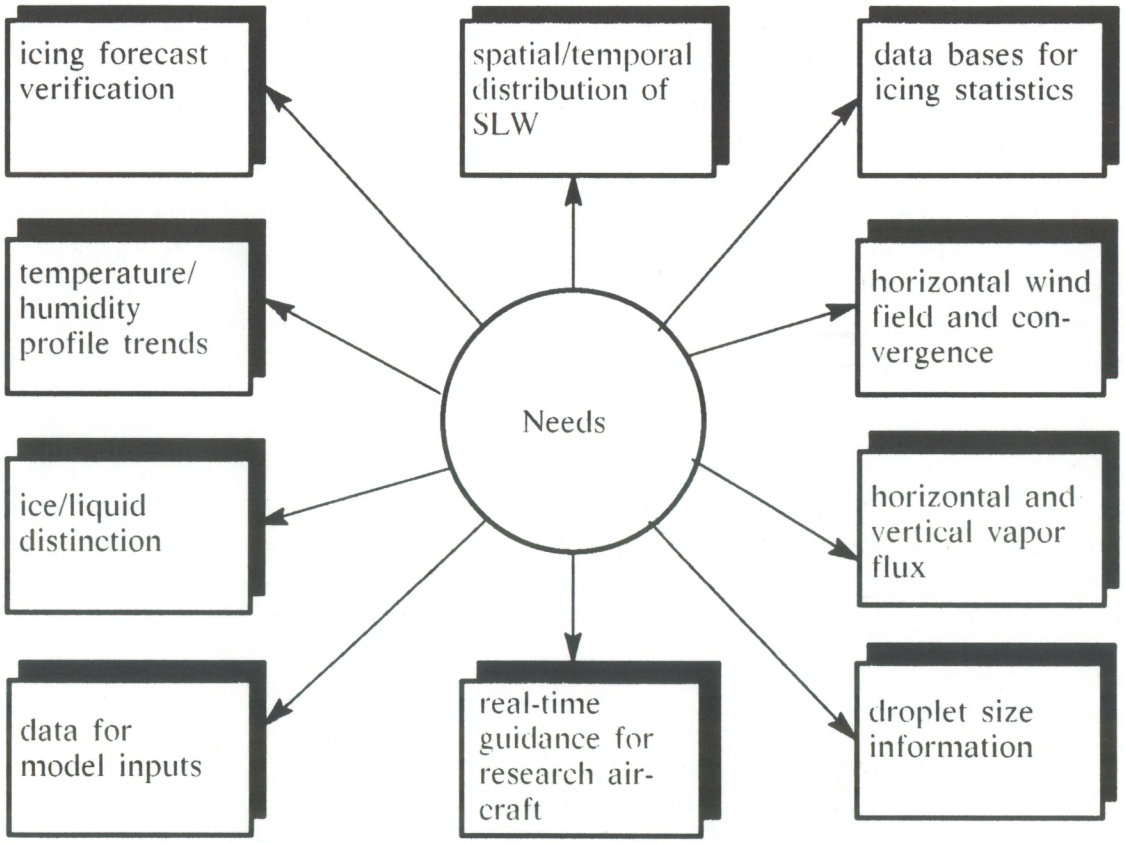

Figure 2.2. Summary of needs to be fulfilled to help solve the problem of aircraft icing.

3. WPL REMOTE SENSING CAPABILITY

In the following subsections, we briefly discuss current WPL remote sensing capabilities that can provide information for the detection and forecasting of aircraft icing conditions. Recent results obtained with these instruments are also discussed. It should be remembered that, for some applications, the value of each of these instruments can be enhanced significantly when the instruments are operated in concert; i.e., they should be considered as a *remote sensing system* for measuring parameters crucial to the development of aircraft icing conditions.

3.1 Microwave Radiometers: Integrated Liquid and Vapor

The energy received by a radiometer tuned to frequencies of 21 or 32 GHz is proportional to the integrated amount of water substance existing along the radiometer antenna beam. A measurement at 21 GHz is about 3 times as sensitive to vapor as a corresponding measurement at 32 GHz; conversely, a measurement at 32 GHz is about 2 times as sensitive to cloud liquid as a measurement at 21 GHz. By making simultaneous measurements at the two frequencies, we can determine the vapor and liquid amounts (Guiraud et al., 1979). Accurate results are obtained when nonprecipitating clouds are observed or during dry snowfall in the absence of melting. Absorption by ice in the microwave region is some 2 orders of magnitude below that by liquid water. As a result, the two-channel radiometer is insensitive to amounts of ice found in the majority of clouds but is capable of measuring vapor and liquid integrated along the beam.

Encouraged by earlier results on the detection of SLW with fixed-beam systems (Hogg et al., 1980; Snider et al., 1980), WPL developed a steerable-beam and transportable dual-frequency radiometer at 20.6 and 31.65 GHz. (Hogg et al., 1983). This instrument has been involved in a variety of experiments that have focused on SLW in winter storms. A summary of its usage, as well as that of other WPL remote sensors, is given in Table 3.1.

The WPL dual-wavelength steerable radiometer has identical and coaxial beams at the two wavelengths. Because the radiometer antenna is arranged to be steerable in elevation and azimuth, the system can provide data on the directional distribution of liquid and vapor surrounding the instrument. We stress that the radiometer measures integrated quantities; the instrument measures the total amount present along each radial direction from the antenna.

Such measurements have been found to be valuable in relating amounts of liquid to terrain features. An example of several azimuth scans made consecutively over a period of about 1.5 h is shown in Fig. 3.1. Statistical examination of scans made during about 15 storms observed in the Tushar Mountains of southwestern Utah show that, on average, maximum liquid is situated above the lift regions of the upwind mountain barrier (Snider et al., 1986). Steerable-beam radiometer observations at Steamboat Springs, Colorado, show a similar consistent maximum above the upwind slopes of a mountain barrier (Rauber et al., 1986; Rauber and Grant, 1986). Clearly, orographic forcing has an important effect upon formation of SLW in mountainous regions.

Table 3.1. Activities in which WPL remote sensors were used to study the morphology of SLW

Activities	Year(s)	Instruments
Aircraft icing detection	1979	WPL dual-wavelength zenith-viewing microwave radiometer
Sierra Cooperative Pilot Project	1980–1981	WPL dual-wavelength steerable-beam microwave radiometer
Colorado Orographic Seeding Experiment (COSE III)	1981–1982	WPL dual-wavelength steerable-beam microwave radiometer
Sierra Cooperative Pilot Project	1982–1983	Dual-wavelength steerable-beam microwave radiometer built by WPL for Bureau of Reclamation
Cooperative Federal/State Weather Modification Project, Beaver, Utah	1983	WPL dual-wavelength steerable-beam microwave radiometer
Aircraft icing detection	1983–1984	WPL dual-wavelength zenith-viewing microwave radiometer
Colorado Orographic Seeding Experiment (COSE IV)	1984–1985	WPL dual-wavelength steerable-beam microwave radiometer
Cooperative Federal/State Weather Modification Project, Beaver, Utah	1985	WPL dual-wavelength steerable beam microwave radiometer and Ka-band Doppler radar
Aircraft icing detection (PROFS)	1987	WPL network of dual-wavelength zenith-viewing microwave radiometers and wind profiling radars
Aircraft icing detection validation	1987–1988	WPL network of dual-wavelength zenith-viewing microwave radiometers, wind profiling radars and color-enhanced GOES images

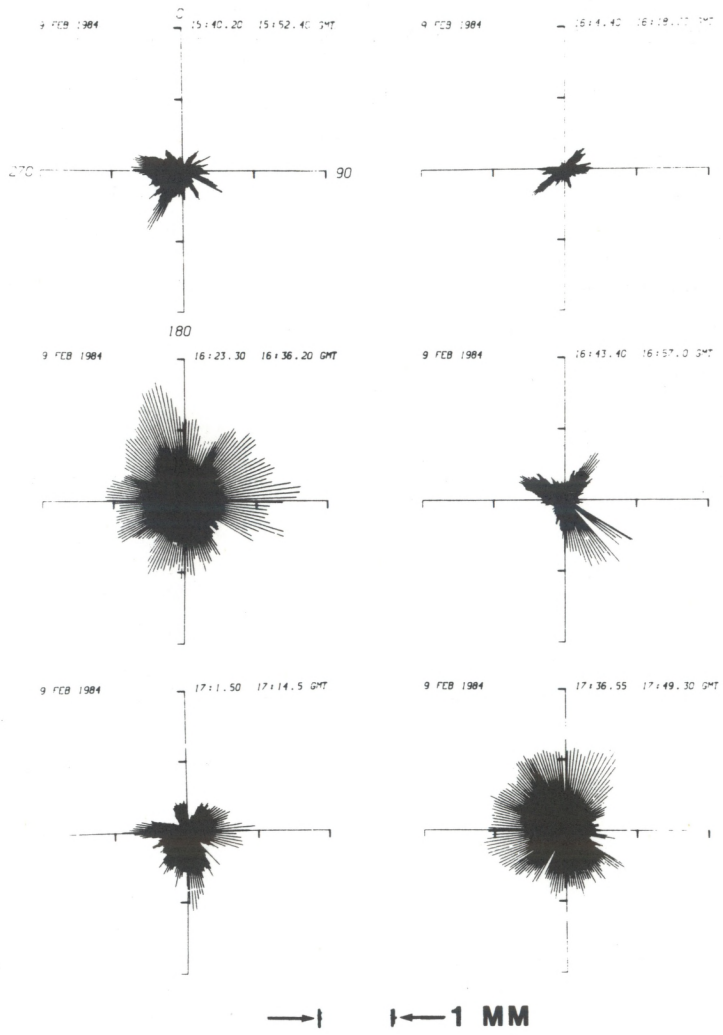

Fig. 3.1. Consecutive azimuth scans at 225° elevation showing the highly variable spatial distribution of liquid water over a mountain barrier near Beaver, Utah. (From Snider et al., 1986.)

An example of the temporal and spatial behavior of SLW during a winter storm is presented in Fig. 3.2. This display, referred to as an "azimuth-time" diagram, is constructed from azimuth scans recorded continuously during storms. It offers a convenient means of presenting the time history and spatial distribution over periods of several hours. The example clearly shows the passage of SLW in two separate events as well as the directional distribution of SLW during the entire storm. Continuous observations such as these have allowed us to relate the behavior of liquid water during storms to synoptic conditions, local convective activity, the occurrence of precipitation, and other meteorological factors. These results suggest that the deployment of such a steerable radiometer at an airport could be useful for routine monitoring of aircraft icing conditions.

The potential of the steerable-beam system for cloud liquid research was enhanced by the addition, in 1987, of a 90.0 GHz channel to the WPL instrument. This channel is a factor of 6 more sensitive to cloud liquid than is the 31.65 GHz channel. Thus the im-

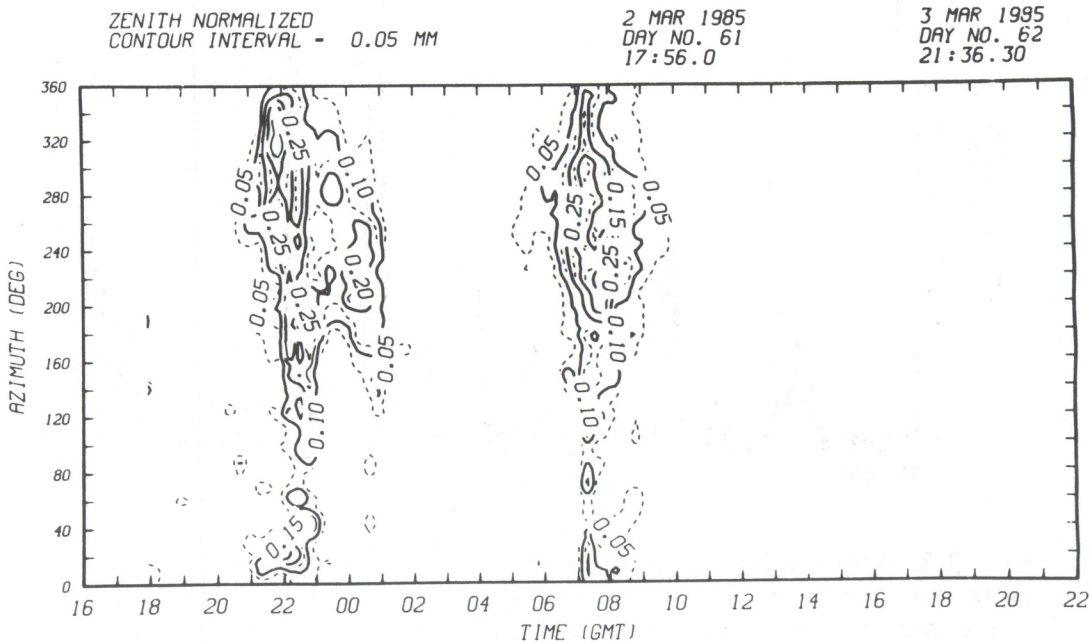

Fig. 3.2. Azimuth-time diagram showing contours of constant SLW during a winter storm. (From Snider et al., 1986.)

proved system can measure integrated liquid water (in units of volume of integrated liquid per unit area) in the range from 0.03 to 5.0 mm. For a uniform cloud of 500 m thickness, these amounts translate to a cloud liquid density of 0.06–10.0 g/m^3 when the cloud is viewed at vertical incidence.

Since the original deployment of the dual-frequency zenith-viewing radiometer at Stapleton Airport in 1979, measurements with this system have been used in a variety of studies relevant to aircraft icing. The most comprehensive of these was by Popa Fotino et al. (1986) in which 2 years of radiometer data were compared with pilot reports of icing. In spite of the difficulties associated with the somewhat sketchy nature of pilot reports, 90% of the reported icing conditions within 10 nmi of the radiometer were identified by the radiometric technique. An example of an aircraft icing index that Popa Fotino et al. (1986) developed is shown in Fig. 3.3; the correlation with pilot reports is excellent.

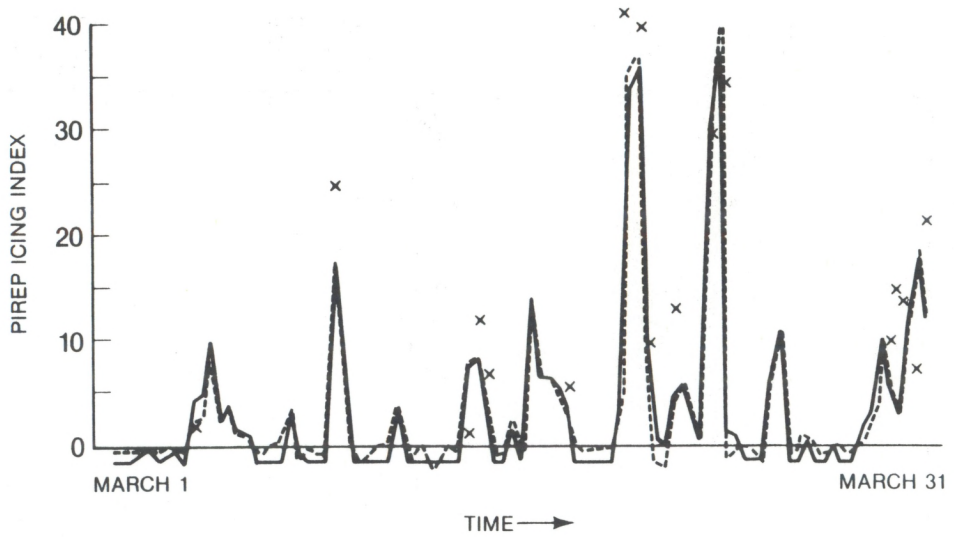

Fig. 3.3. Aircraft icing index: × is from pilot reports, the dashed line is from seven surface measurements, and the solid line is from radiometric liquid measurement only. (From Popa Fotino et al., 1986.)

3.2 Scanning Pulsed-Doppler Radars: Dynamic Forcing of SLW

WPL has designed and built two 3.2-cm-wavelength (X-band) and one 8.6-mm-wavelength (Ka-band) Doppler radars for cloud physics research. Given that one of the main forcing mechanisms for SLW is the vertical air motion, as explained in Section 2, these radars are especially useful during icing experiments for documenting the mesoscale velocity and reflectivity structure. All three radars are computer controlled with a versatile radar control computer program, real-time data processors, and color displays. One of the X-band radars and the Ka-band radar also have dual-circular polarization capability; circular depolarization ratio (CDR) is displayed along with Doppler velocity and reflectivity. Table 3.2 summarizes a few of their characteristics.

Table 3.2. Scanning pulsed-Doppler radar specifications

Characteristics	X-band	Ka-band
Frequency (GHz)	9.3	35.0
Peak power (kW)	40	100
Pulse duration (μs)	0.75 (110 m)	0.25 (37 m)
Beamwidth (deg)	0.8	0.5
Minimum reflectivity at 10 km (dBZ)	−18	−27

3.3 Microwave Radiometer and Ka-Band Doppler Radar: Vapor Flux

A recurring theme of this report is that data from individual remote sensors can be combined to derive new products not attainable from the individual sensors alone. An excellent example of such a combination is water vapor flux, derived using data from WPL's Ka-band Doppler radar and the steerable-beam radiometer. Wind profiles derived from the Ka-band radar are combined with simultaneous observations of water vapor density profiles by a microwave radiometer to produce continuous measurements of water vapor flux normal to the mountain range. Details of the method are given in Snider et al. (1986) and Uttal et al. (1989).

Comparison of temporal variations of water vapor flux and integrated liquid water in the Tushar Mountains of central Utah shows that maxima in water vapor flux normal to the mountain barrier were closely associated with maxima in SLW and may have actually preceded maxima in SLW by about an hour. Figure 3.4 presents this behavior for one case study. The figure also shows the behavior of liquid water relative to frontal passage, precipitation, and the amount of riming occurring at the remote sensing site. The extent to which this situation generally occurs in orographic clouds has yet to be determined. However, the finding does suggest the possibility that a microwave radiometer and Doppler radar located upwind of a mountain barrier may be able to indicate the onset of SLW and therefore predict optimum times for cloud seeding or forecast conditions favorable for aircraft icing.

3.4 Doppler and Multiwavelength/Incoherent Lidars: Winds, Temperature and Water Vapor

WPL currently operates two lidar systems that could be used in icing-related experiments. Specifications for the two systems are given in Table 3.3. Each of the systems is transportable and possesses unique characteristics for the study of atmospheric processes. The pulsed-Doppler lidar system provides range-resolved information on wind velocity and aerosol structure to ranges of 15–30 km. It has been employed in a number of original field experiments in recent years, including characterization of gust structure during downslope windstorms, measurement of cirrus cloud properties and depolarization, identification of low-reflectivity microbursts, and observation of mesoscale wind and aerosol structure associated with air pollution events in the Denver metropolitan area.

A completely different system, the multiwavelength incoherent lidar, measures intensity of signals backscattered from aerosol and cloud particles at several different wavelengths. It has been used primarily for investigation of aerosol plume dispersion in recent years, but it could be modified to measure temperature and water vapor using Raman lidar techniques. Because the system has a dual-polarization capability, it can be used to provide information on icewater content near cloud base such as the measurements reported by Sassen (1986). He has shown that the depolarization ratio computed from cloud-backscattered lidar signals can be used to detect the presence of ice or SLW. Low values (<0.15) generally represent water-dominated cloud conditions; increasing values of the depolarization ratio indicate increasing relative ice content in the cloud region.

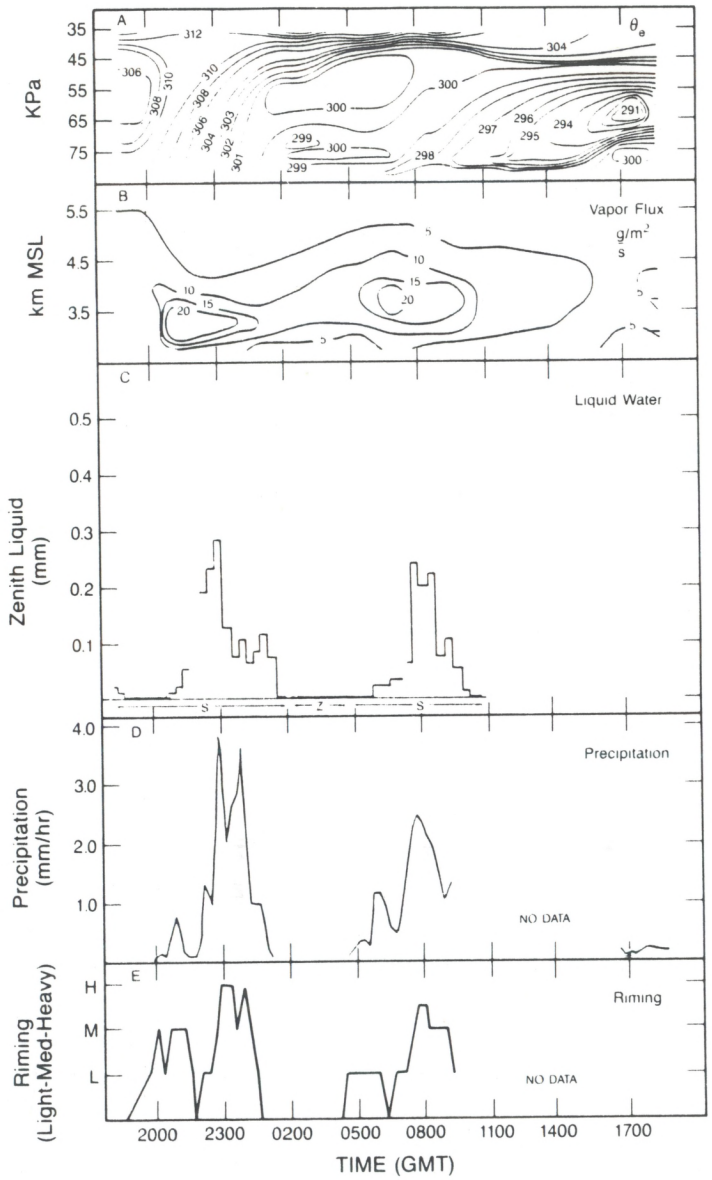

Fig. 3.4. Time series of equivalent potential temperature (θ_e), water vapor flux, liquid water content, precipitation rate, and riming for March 2–3, 1985, at Beaver, Utah. The water vapor flux values were derived using data from WPL's Ka-band Doppler radar and microwave radiometer. (From Uttal et al., 1989.)

Table 3.3. Operating characteristics of WPL lidar systems.

Characteristic	Pulsed Doppler	Multiwavelength incoherent
Wavelength (μm)	10	0.347, 0.532, 0.694
Range resolution (m)	150 or 300	6.0
Quantities measurable	Wind speed, aerosols, clouds, potential for water vapor and O_3	Aerosols, clouds, water vapor (planned)
Depolarization ratio	Planned	Existing only at 0.694
Scannable beam	Yes	Yes
Optics diameter (m)	0.28	0.70
Pulse repetition frequency (Hz)	20	0.5 (0.347, 0.694) 10 (0.532)
Energy per pulse (J)	0.5	0.3 (0.347), 0.15 (0.532), 2 (0.694)

3.5 Dual-Frequency Radar: SLW Mapping

The attenuation experienced by a beam of microwave energy is directly proportional to the amount of liquid along its path. This suggests a method for measuring liquid within a cloud by simultaneously transmitting two frequencies, one chosen so that it is measurably attenuated and the other chosen to be weakly attenuated. This possibility was first mentioned by Atlas (1954) and proposed later for rain measurements by Goldhirsh and Katz (1974). We examine here the possibility of using 35 GHz (Ka-band) and 9.3 GHz (X-band) as the attenuating and weakly attenuating frequencies, respectively, to measure in-cloud SLW in amounts that are hazardous to aircraft.

Given the expected SLW content in hazardous icing conditions and the known attenuation coefficients due to liquid water, we expect that there should indeed be a small but measurable attenuation signature at Ka-band relative to a weakly attenuating X-band reference signal. The relatively small amounts of SLW that are expected in these clouds with icing hazard potential make this wavelength combination ideal; longer wavelengths than Ka-band would not attenuate enough to produce a detectable signature, and shorter wavelengths than Ka-band would have complications from Mie-scattering effects. The Ka-band

and X-band one-way attenuation coefficients from Battan (1973) are given in Table 3.4 for water and ice.

Characteristics of clouds that produce hazardous icing conditions have been summarized by Politovich (1989), who indicated an average SLW content of about 0.2 g/m^3 within clouds that produce significant aircraft icing. Vogel (1988) reported that light icing can occur in stratiform clouds with SLW content in the range from 0.12 to 0.68 g/m^3. He also reported that moderate icing intensity occurs in stratiform clouds when SLW is in the range from 0.69 to 1.33 g/m^3. If we assume an SLW content of 0.2 g/m^3 and use the attenuation coefficients in Table 3.4 we can determine the expected attenuations (in dB/km) for rather minimal icing potential. We also assume an ice mass content of 2 g/m^3 to compute the expected one-way attenuations at the two frequencies being considered. The expected one-way attenuations for these assumed densities for water and ice are given in Table 3.5.

The values in Table 3.5 show that ice would produce negligible attenuation at either frequency. However hazardous amounts of SLW would produce two-way attenuation of almost 0.5 dB/km at Ka-band and an order of magnitude less attenuation at X-band. A remote sensing system composed of colocated Ka-band and X-band radars with electrically-slaved antennas should be able to detect attenuation-caused reflectivity differences when the radars perform identical scans. This is especially true if regions of SLW extend over the horizontal distances of 5–10 km that produce an icing hazard. This is not an unreasonable expectation in view of the results of Sand et al. (1984), who found that, on the average, a 5 km continuous exposure to SLW exceeding 0.2 g/m^3 was encountered once in about 2 h of flying during research missions with the University of Wyoming King Air aircraft.

Given these considerations, it is straightforward to show that the amount of SLW can be expressed in terms of the received power at the two frequencies as follows:

$$M = (4.38/D) \log \{P_K(r)P_X(r + D)/[P_K(r + D)P_X(r)]\} \qquad (1)$$

Table 3.4. One-way attenuation coefficients

	Ka-band (dB/km)/(gm/m^3)	X-band (dB/km)/(gm/m^3)
Water (–8°C)	1.250	0.112
Ice (–10°C)	0.00291	0.000819

Table 3.5. One-way attenuation

	Ka-band (dB/km)	X-band (dB/km)
Water	.237	.021
Ice	.006	.002

where M is the liquid water content (in g/m^3), P_K is the power received by the attenuating Ka-band radar, P_X is the power received by the weakly attenuating X-band radar, r is range, and D is the range interval over which the value of M is averaged. No assumptions are made about the uniformity of radar reflectivity or the droplet size distribution. The technique is unaffected by errors in the radar constant or attenuation occurring at range less than r.

3.6 Wind-Profiling Radars: All-Weather, Continuous Wind Profiles

As discussed in Section 2.2, knowledge of the vertical profiles of horizontal and vertical winds is essential to forecasting of SLW. In addition, it is known that shear layers during stratus conditions can enhance icing potential by producing larger water droplets. Since 1982, WPL has constructed and operated various wind-profiling radars; their characteristics are given in Table 3.6. These radars operate in all weather conditions and make use of backscatter from small-scale (one-half radar wavelength) refractive index fluctuations in the atmosphere.

The *transportable* 405-MHz wind profiler that was developed and tested by WPL has coverage through the lower 6 km (Moran et al., 1989). An example of data produced by

Table 3.6. Characteristics of WPL wind-profiling radars

Characteristic	49.92 MHz	404.37 MHz	915 MHz
Location	Platteville	Transportable	Stapleton
Peak power (kW)	27	1.2	5.6
Average power (kW)	180	30, 45	110
Pulse width (μs)	2, 16	1, 3	1
Antenna aperture (m × m)	100 × 100	5.5 m diameter	10 × 10
Minimum range (km)	2	0.4	0.3
Expected range (km)	12, 18	7	6
Range resolution (km)	0.3, 2.4	0.15, 0.45	0.15

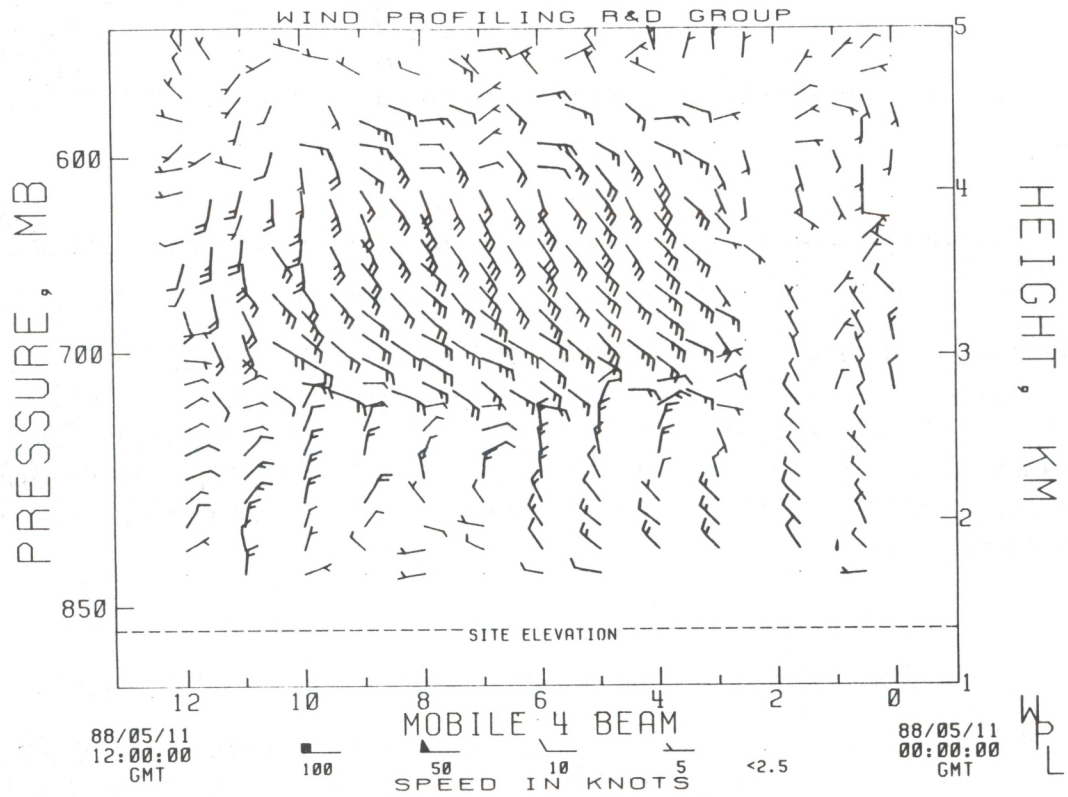

Fig. 3.5. A 12-h wind profile from a lower-tropospheric transportable profiler at Fort Huachuca, Arizona, May 11, 1988. Onset of a mid-level jet occurred at 0300 UTC, and the jet continued until 1000 UTC. (From Moran et al., 1989.)

this radar is shown in Fig. 3.5. Because of its transportability and its scanning capability, the system seems ideal for many experimental studies of cloud liquid.

3.7 Radio Acoustic Sounding System: Temperature Profiling

RASS is a promising method for sensing temperature profiles by combining radar and acoustic techniques (May et al., 1988). This method, as employed by WPL, uses a wind-profiling radar together with a wide-bandwidth acoustic source. By measuring the frequency at which the acoustic and radar waves are Bragg-matched (the acoustic wavelength being equal to half the radar wavelength), RASS measures the speed of sound and hence the virtual temperature. During periods in which vertical air motion occurs, vertical velocity corrections are necessary and can be easily performed with this system from the vertically pointing radar beam. Currently, temperature profiles accurate to better than 0.7°C have been derived using RASS with the WPL wind-profiling radars operating at 50, 405, and 915 MHz. Examples of temperature profiles derived by this technique are given in Fig. 3.6, and a summary of operating characteristics is given in Table 3.7.

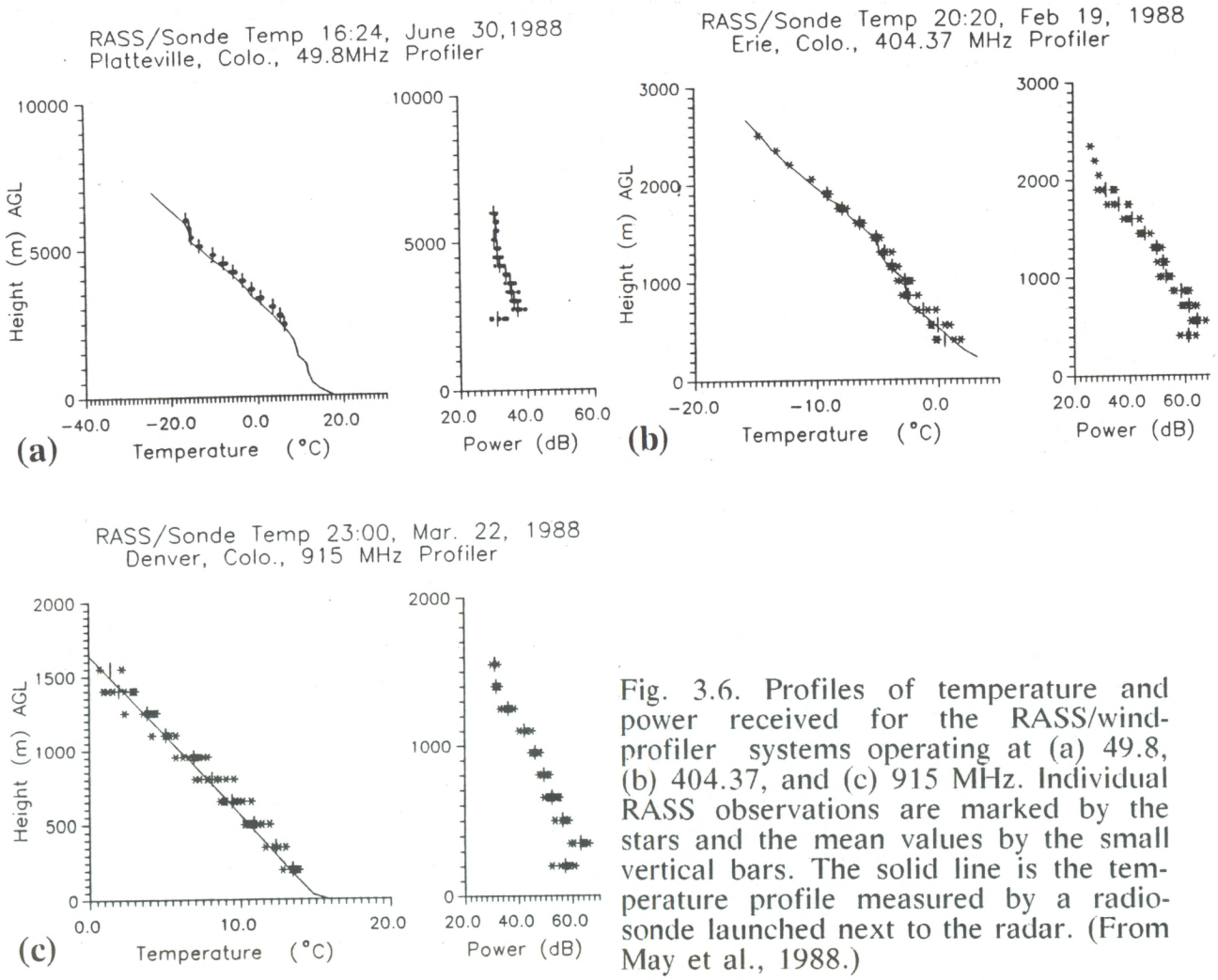

Fig. 3.6. Profiles of temperature and power received for the RASS/wind-profiler systems operating at (a) 49.8, (b) 404.37, and (c) 915 MHz. Individual RASS observations are marked by the stars and the mean values by the small vertical bars. The solid line is the temperature profile measured by a radiosonde launched next to the radar. (From May et al., 1988.)

It is certain that RASS will be an important supplement to other sensors. For example, if cloud base is above the freezing level, the combination of RASS, a ceilometer, and amicrowave radiometer could unambiguously detect supercooled cloud liquid water. In addition, the high-resolution temperature profiles from RASS can be used as input to forecast models or to other predictive schemes. One example is the Minus-8D technique, which identifies layers of rime icing potential from radiosonde temperature and moisture soundings (Tucker, 1983). We discuss this further in Section 4.2.

Table 3.7. Characteristics of RASS/wind-profiler systems operating at three sites

Characteristic	Platteville	Erie	Denver
	Radar		
Frequency (MHz)	49.8	404.37	915
Wavelength (m)	6.0	0.7414	0.3
Antenna size (m^2)	10,000	25	100
Beamwidth, 1 way (deg)	3	7.8	2
Range resolution (m)	300	150	150
Mean power (W)	200	30	100
Sampling time for 1 profile (min)	1	1	1
	Acoustic		
Frequency (Hz)	~110	~900	~2000
Beamwidth, 1 way (deg)	~60	~17	~8
Acoustic power (W)	50	5	5
	RASS Altitude Coverage		
Min. altitude (km)	2.1	0.4	0.2
Max. altitude (km)	5–9	1.5–2.5	0.7–1.5
Observation period (1988)	May-Jun	Jan-Feb	Mar-Apr

3.8 Infrared Radiometers: Cloud-Base Temperature

Two infrared radiometers have been acquired by WPL for use in cloud studies. These radiometers are Barnes PRT–5 instruments that operate at 10.6 μm wavelength with a 1.0 μm bandwidth. The instruments were acquired to supplement existing microwave radiometers, and the design and fabrication of the housing of these units is compatible with those of the microwave systems. Initial experience with these instruments indicates that they can unambiguously differentiate between clear and cloudy conditions and that, together with the microwave radiometers, they can differentiate between ice and liquid clouds. In addition, the combined infrared-microwave system may be able to measure cloud-base temperature of liquid-bearing clouds to 1°C (Snider, 1988). An example of data from infrared and microwave radiometers is shown in Fig. 3.7.

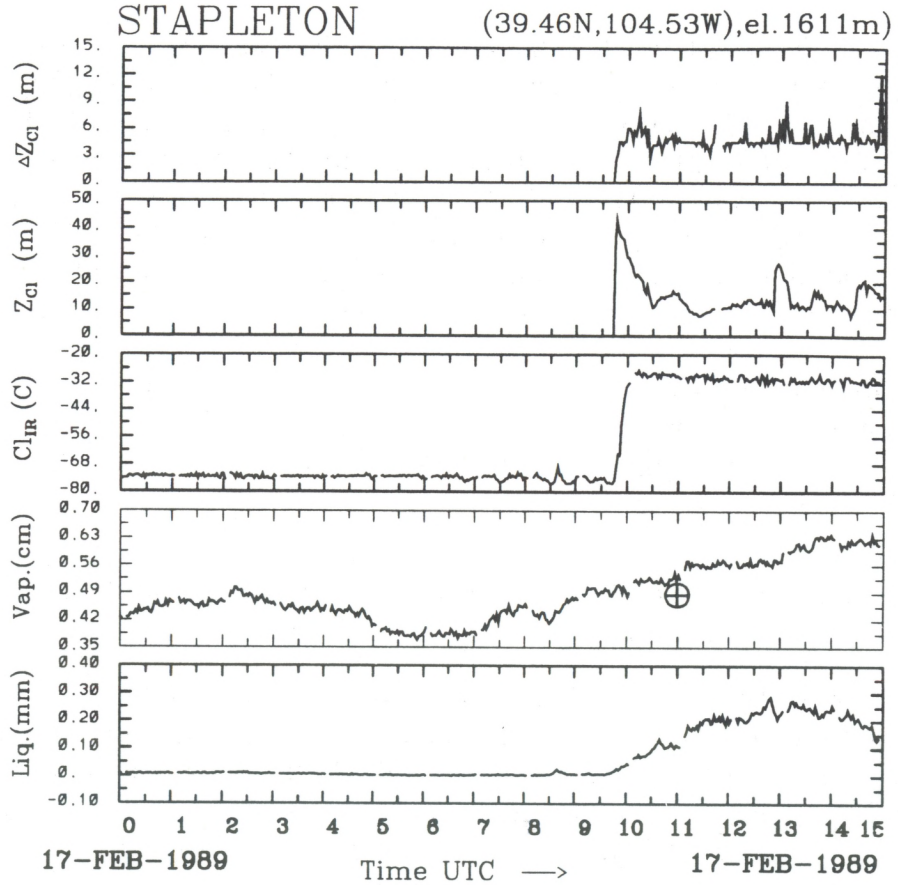

Fig. 3.7. Time series of cloud thickness, cloud base height, cloud base temperature, precipitable water vapor, and integrated cloud liquid.

3.9 Ceilometers: Cloud-Base Height

The capability to measure cloud-base height (CBH) is important for many applications including aviation (Eberhard, 1986). Measurements of CBH by the new-generation National Weather Service (NWS) lidar ceilometers have also proved to be useful in cloud radiation research (Snider, 1988). Data from one of these instruments at Stapleton Airport are now being routinely collected by WPL. Figure 3.7 shows NWS ceilometer CBH data displayed with other products giving cloud information. Together with measurements of the vertical temperature profile, such as provided by RASS, and cloud liquid water, as provided by the microwave radiometers, the CBH measurements could help identify supercooled clouds. In addition, information on the horizontal distribution of CBH could easily be provided by the WPL scanning lidar operating either in the conical-scan or the range height indicator (RHI) mode. Such measurements would be of benefit to many cloud research efforts.

3.10 GOES Images: Cloud-Top Temperature

The Geostationary Operational Environmental Satellite (GOES) visible and infrared images provide a useful supplement to the quantitative data provided by surface-based

remote sensors. Consequently, WPL has developed a workstation to process, display, and analyze GOES data. The workstation currently uses data operationally acquired by NOAA's Program for Regional Observing and Forecasting Services (PROFS). The computer software that will display GOES data tapes from the National Environmental Satellite, Data, and Information Service (NESDIS) is nearing completion. The GOES images are useful in determining the geographical distribution of clouds, and, in some cases, in determining cloud-top temperatures. Such information can benefit both real-time operations and post-experiment data analyses. The images were of substantial benefit in relating ground-based measurements of cloud liquid water at a single location to a wider geographical distribution of aircraft icing reports (Decker et al., 1986). In a later study, icing hazard altitudes identified by combining GOES cloud top temperatures with ceilometer and microwave radiometer measurements were verified by instrumented aircraft (Popa Fotino et al., 1989).

3.11 Aircraft Zenith-Viewing Dual-Channel Microwave Radiometer: Horizontal Distribution of SLW

Horizontal distribution of cloud liquid water could be measured using an upward-looking microwave radiometer mounted on an aircraft. Such a system could fly both under and through regions of supercooled liquid. At all flight levels, the amounts of water vapor and cloud liquid above the aircraft could be measured. If the aircraft were also equipped with cloud microphysical instruments, a variety of research opportunities would be available. With these opportunities in mind, WPL has designed, and partially constructed, a dual-channel microwave radiometer for ultimate deployment on the NOAA P–3 aircraft (Fedor et al., 1988).

4. PROPOSED EXPERIMENTS AND APPLICATIONS

4.1 Verification of Dual-Frequency Radar Technique to Measure SLW

The dual-frequency radar technique to measure the spatial distribution of SLW could have enormous practical impact, certainly for identifying SLW (Section 3.6) in the vicinity of airports, but also as a possible onboard technique for use in aircraft. Therefore, testing of this technique is a high priority.

One experiment that we suggest is to perform identical low-elevation conical scans with colocated X-band and Ka-band radars, and to use Eq. (1) to compute SLW at elevations above the freezing level. If precipitation exists, the freezing level is usually obvious from the bright band that appears in the reflectivity field and even more obvious in the field of circular depolarization ratio (CDR) available from the two WPL radars. Otherwise the freezing level would be known from a RASS or from a radiosonde.

The two radar antennas would be electrically slaved together, and the radars and data processors supplied with common triggers. Pulse widths would be matched as closely as possible. Potential problems with unmatched beamwidths (Ka-band = 0.5°, X-band =

0.8°) are somewhat uncertain but are expected to be far less of a problem than they have been for the dual-wavelength techniques used for hail detection, for example. Spatial gradients in hail storms are much more severe than we would expect for the more stratiform (upslope) condition in which hazardous icing occurs in eastern Colorado.

The radars would be colocated at the WPL Erie site, 6 km north of the Boulder Atmospheric Observatory (BAO) tower, as shown in Fig. 4.1. Having the BAO tower in view from this site would present an excellent opportunity to verify the antenna alignment by scanning across the tower with the antennas slaved together when microwave sources are in place on the tower. Dynamic misalignments as small as 0.2° should be evident in such a test.

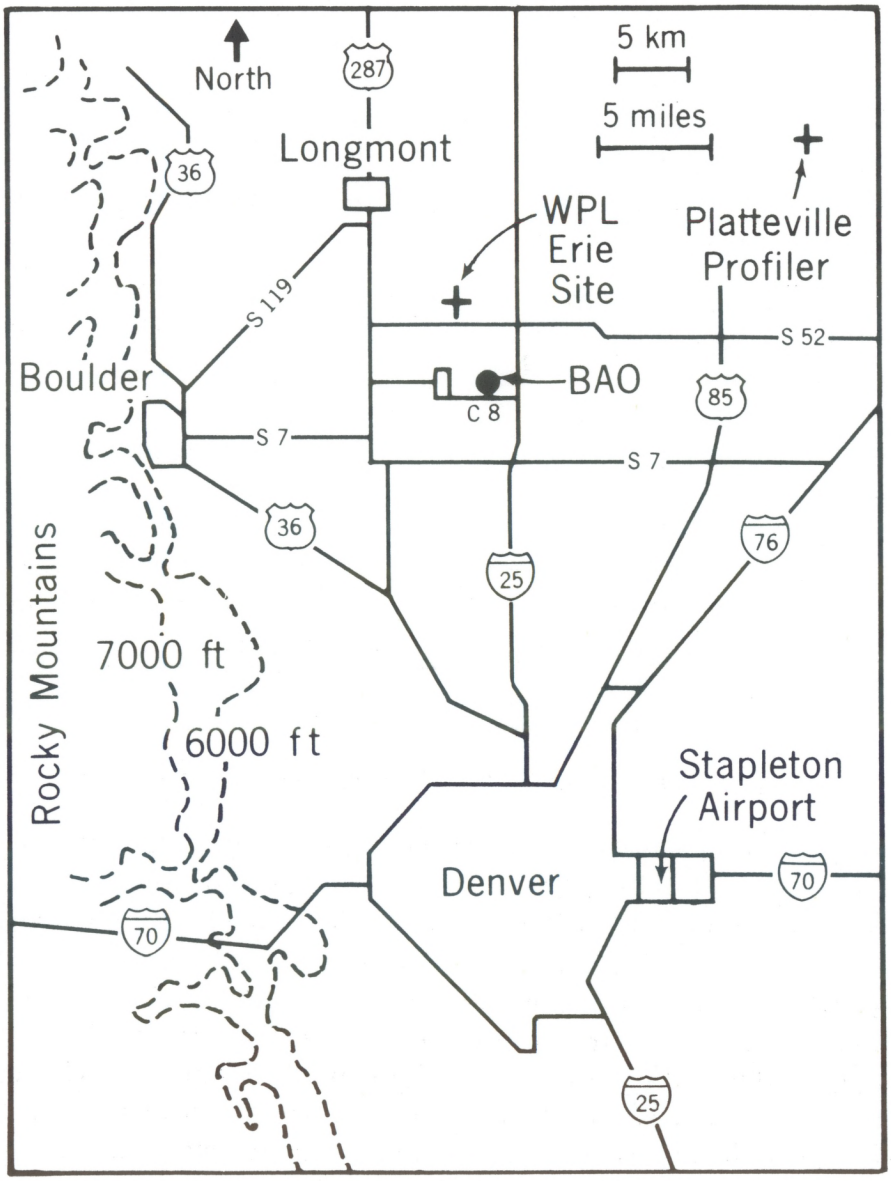

Fig. 4.1. Map of proposed icing research site in northeast Colorado.

It is believed that SLW generally occurs in regions with small amounts of ice and that the SLW droplets are generally small; therefore low reflectivities are anticipated in the regions of interest. This raises the question of radar sensitivity because, in order for attenuation to be measured, echo from the SLW region must be received by both radars. The minimum reflectivity observable by the NOAA Ka-band (log channel) radar at Beaver, Utah, was -26 dBZ at a range of 4 km, which translates to a -8 dBZ minimum detectable reflectivity at 32 km. The WPL X-band radar is about 10 dB less sensitive to hydrometeors, so echoes of about 0 dBZ should be observable by both radars out to about 30 km. The use of linear receivers for the weakest signals would extend the workable range by at least a factor of 2, since the linear receivers are about 8 dB more sensitive than the log receivers for these radars.

Real-time color displays of the Ka-band/X-band reflectivity ratio, or better yet, its range derivative, could be used to vector research aircraft, if they are available, into suspected hazardous icing regions. The NOAA P-3 aircraft, with its complement of particle-measuring and liquid-sensing probes, would be an ideal candidate to probe suspect clouds, particularly if the multichannel microwave radiometer were installed. Doppler velocity fields could provide information about low-level convergence as an aid in establishing the ability of radial velocity features to signify updraft-forced SLW regions.

The WPL Erie site is 27 km and 40 km from the Platteville and Stapleton profilers, respectively, both of which have vertically pointing radiometers for integrated liquid measurements. Data from these systems would be useful in providing verification of the differential attenuation measurements of SLW in the absence of rain. The WPL steerable-beam, transportable three-channel radiometer would be located at the BAO and used in a sector-scan mode. It would probe regions suspected (from the differential attenuation display) of having SLW. RASS would be used in real time at the BAO with the 405 MHz wind profiling system to determine temperature profiles to 3 km for identification of the freezing level. The height of the -15°C level, the level above which icing is unlikely to occur, would also be useful in identifying possible false alarms that might appear in the differential attenuation display.

4.2 Remote Sensing Inputs to Icing Forecast Algorithms

The temporal continuity offered by remote measurements can enhance the effectiveness of existing techniques that use radiosonde measurements, usually available only every 12 hours. The Minus-8D technique, which identifies layers of rime icing potential from radiosonde temperature and dewpoint soundings, is an example of an existing technique (Tucker, 1983). Figure 4.2 shows the results when the technique was applied to two radiosonde soundings, whose launch times are marked by vertical dashed lines; no icing hazard was indicated by the Minus-8D technique in either sounding. However, application of the technique to radiometrically-determined temperature and humidity soundings, available every 20 min, revealed layers of rime icing potential; they are spanned by the vertical bars in the figure. The dark circles identify altitudes at which pilots reported aircraft icing within a 50 nmi radius of the radiometer. A technique that was useless in

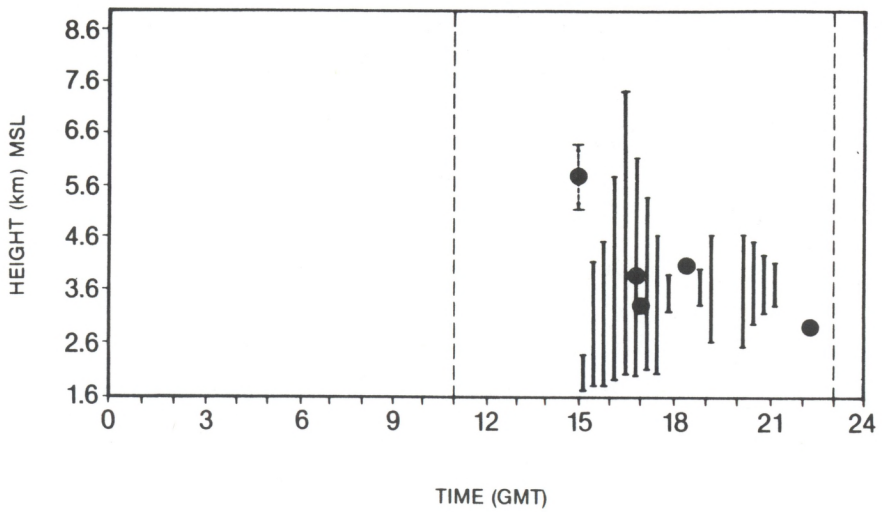

Fig. 4.2. Icing hazard altitudes identified by applying the Minus–8D method to radiometric soundings at 20-min intervals on March 16, 1984 (solid vertical bars). Dashed lines mark radiosonde launch times. Circles show altitudes and times of icing events reported by pilots within 50 nmi of the radiometer. (From Decker et al., 1986.)

detecting this icing event when it was applied to conventional measurements proved to be very successful when it was applied to continuous remote measurements.

This example is not an isolated incident. Thirteen out of 16 reported aircraft icing incidents within 20 nmi of the radiometer occurred within the icing hazard altitude range identified by applying the Minus–8D technique to the radiometric soundings. Only a dedicated aircraft can conclusively validate this technique.

With the existing and planned facilities of WPL at Stapleton Airport and at Platteville, the Minus-8D technique could be tested for an entire winter season if a dedicated research aircraft were available. These facilities will include, on a quasi-operational basis, the six-channel microwave radiometer and the 915 MHz RASS at Stapleton, and a dual-channel microwave radiometer and a 405 MHz RASS at Platteville. Other prediction algorithms, as long as they are based on conventional profiles of temperature, humidity, and winds, could also be routinely tested.

4.3 National Program to Improve Aircraft Icing Forecasts

Hinkelman (1989) recently summarized the national program (Federal Coordinator, 1986) for developing the capability to detect, monitor, and forecast icing conditions through the use of research aircraft and new remote sensing technology. Included in this plan is the use of several WPL remote sensors, including zenith-viewing microwave radiometers and wind profilers. However, because the program was designed in 1986, several of the new technologies described here were not considered. We comment briefly on how our new technologies relate to the following tasks outlined by Hinkelman:

In-situ detection of icing conditions. The inclusion of the aircraft-mounted dual-frequency radiometer, if used in conjunction with cloud microphysics instrumentation, could add significantly to the in-situ detection capabilities. By flying at several levels below and within a cloud, the aircraft could measure the amount of liquid above it. This amount could be correlated both with measured cloud microphysical parameters and actual aircraft icing.

Remote detection and monitoring of icing condition. Included in Hinkelman's paper are Doppler radars, zenith-viewing microwave radiometers, and satellite sensors. The steerable-beam radiometer, RASS, and NWS lidar ceilometers could add valuable information to this data base. Other sensors, notably the lidar and the dual-frequency radar, if they could be run routinely, would also be valuable. The presence of the dual-frequency radiometer on an aircraft could also be used here for validation.

Acquisition and analysis of meteorological and microphysical data. Suitable deployment of all of the remote sensors mentioned in this report could add significantly to the planned data base.

Development and evaluation of forecasting techniques. Some of the quasi-operational devices, such as the wind profiler and the zenith-viewing dual-frequency radiometer, will be used in the development of forecasting techniques. However, RASS, the steerable-beam radiometer, and cloud-base height and temperature measurements, could provide valuable data, both for input to and for evaluation of forecasting techniques. Again, an aircraft radiometer could help in forecast technique validation.

In summary, although some of WPL's sensors are included in the National Program to Improve Aircraft Icing Forecasts, it is clear that some recently developed sensors and concepts could also provide significant impact to many areas of this program.

5. SUMMARY

The development of remote sensing techniques by the Wave Propagation Laboratory has occurred steadily over the years; a primary focus has been on measuring variables useful in meteorological forecasting. The thrust of this report is that many of these techniques, operating in concert, can have an important role in identifying and forecasting aircraft icing conditions. Most of the meteorological parameters that significantly affect the icing of aircraft can be measured by these remote sensing techniques.

Figure 5.1 summarizes current techniques available at WPL that can be applied to this problem. It is significant that many of these observations, such as from wind profilers, RASS, and microwave radiometers, can be made routinely, in nearly all weather conditions, by unattended instruments. Some of the newer techniques, such as lidar and dual-frequency radar, currently require skilled operators, but can provide a wealth of information for research and, ultimately, operational use. Another new technique, the dual-chan-

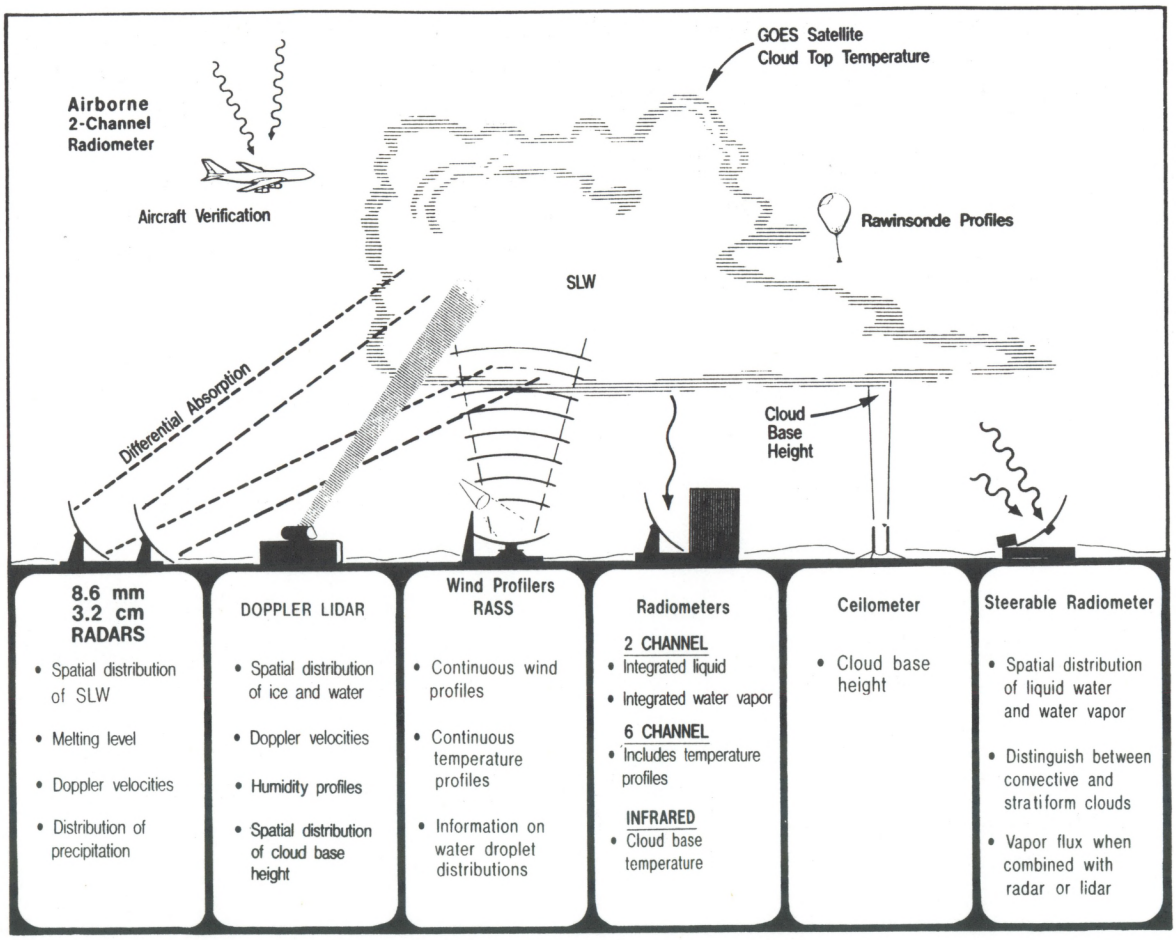

Fig. 5.1. The combined capabilities of Wave Propagation Laboratory remote sensing instruments for measuring supercooled liquid water.

nel radiometer on an aircraft, could provide previously unattainable information on the horizontal distribution of cloud liquid. Thus, the application of state-of-the-art remote sensing techniques described in this report could lead to significant advances in solving the long-standing problem of forecasting and detecting aircraft icing conditions.

6. ACKNOWLEDGMENTS

Significant contributions have been made to this report from many of our colleagues at WPL. They include R. Reinking, A.J. Bedard, J.B. Snider, T. Uttal, B.E. Martner, J.A. Schroeder, M.T. Decker, B.B. Stankov, and R.M. Hardesty.

7. REFERENCES

Atlas, D., 1954: The estimation of cloud parameters by radar. *J. Meteorol.*, **11**, 309–317.

Battan, L.J., 1973: Radar Observations of the Atmosphere. The University of Chicago Press, Chicago, 324 pp.

Committee Report, 1985: Proceedings, 7th Annual Workshop on Meteorological and Environmental Inputs to Aviation Systems, University of Tennessee Space Institute, Tullahoma, TN, October 26–28, 1983. NASA Conference Publication 2388, 153 pp.

Czekalski, L., 1985: Overview of FAA's Aircraft Icing Program. Proceedings, 7th Annual Workshop on Meteorological and Environmental Inputs to Aviation Systems, University of Tennessee Space Institute, Tullahoma, TN, October 26–28, 1983. NASA Conference Publication 2388, 30–34.

Decker, M.T., I.A. Popo Fotino, and J.A. Schroeder, 1986: Remote detection of aircraft icing conditions using microwave radiometers. NOAA Tech. Memo. ERL WPL–137, NOAA Wave Propagation Laboratory, Boulder, CO, 40 pp.

Eberhard, W.L., 1986: Cloud signals from lidar and rotating beam ceilometer compared with pilot ceiling. *J. Atmos. Oceanic Technol.*, **3**, 499–512.

Federal Coordinator for Meteorological Services and Supporting Research, 1986: National Icing Technology Plan. FCM–P20–1986, Office of the Federal Coordinator, 11426 Rockville Pike, Suite 300, Rockville, MD, 20852, 24 pp.

Fedor, L.S., M.D. Jacobson, A.J. Bedard, Jr., E.R. Westwater, D.C. Hogg, and R.T. Nishiyama, 1988: Dual-channel microwave radiometer for airborne meteorological applications. NOAA Tech. Memo. ERL WPL–157, NOAA Wave Propagation Laboratory, Boulder, CO, 29 pp.

Goldhirsh, J., and I. Katz, 1974: Estimation of raindrop size distributions using multiple wavelength radar systems. *Radio Sci.*, **9**, 439–446.

Guiraud, F.O., J. Howard, and D.C. Hogg, 1979: A dual-channel microwave radiometer for the measurement of precipitable water vapor and liquid. *IEEE Trans. Geosci. Electron.*, **GE-17**, 129–136.

Hansman, J.R., Jr., 1989: The influence of ice accretion physics on the forecasting of aircraft icing conditions. Preprints, 3rd Int. Conf. on Aviation Weather Systems, Anaheim, CA. AMS, Boston, 154–158.

Hinkelman, J.W., Jr., 1989: An overview of the national program to improve aircraft icing forecasts. Preprints, 3rd Int. Conf. on Aviation Weather Systems, Anaheim, CA, 443–445.

Hogg, D.C., F.O. Guiraud, and E.B. Burton, 1980: Simultaneous observations of cool cloud liquid by ground-based microwave radiometry and icing of aircraft. *J. Appl. Meteorol.*, **19**, 893–895.

Hogg, D.C., F.O. Guiraud, J.B. Snider, M.T. Decker, and E.R. Westwater, 1983: A steerable dual-channel microwave radiometer for measurement of water vapor and liquid in the troposphere. *J. Appl. Meteorol.*, **22**, 789–806.

May, P.T., R.G. Strauch, and K.P. Moran, 1988: The altitude coverage of temperature measurements using RASS with Wind Profiler radars. *Geophys. Res. Lett.*, **15**, 1381–1384.

Moran, K.P., R.G. Strauch, K.B. Earnshaw, D.A. Merritt, B.L. Weber, and D.B. Wuertz, 1989: Lower tropospheric Wind Profiler. Preprints 24th Conf. on Radar Meteorology, March 27-31, 1989, Tallahassee, FL. AMS, Boston, 728–731.

Politovich, M., 1989: Measurements of hazardous icing conditions. Preprints, 3rd Int. Conf. on Aviation Weather Systems, Anaheim, CA. AMS, Boston, 159–163.

Popa Fotino, I.A., J.A. Schroeder, and M.T. Decker, 1986: Ground-based detection of aircraft icing conditions using microwave radiometers. *IEEE Trans. Geosci. Remote Sens.*, **GE-24**, 975–982.

Popa Fotino, I.A., M.K. Politovich, and J.W. Hinkleman, Jr., 1989: Aircraft icing conditions detected by combined remote sensors: a preliminary study. Preprints, 3rd Int. Conf. on Aviation Weather Systems, Anaheim, CA. AMS, Boston, 173–177.

Rauber, R.M. and L.O. Grant, 1986: The characteristics and distribution of cloud water over the mountains of northern Colorado during wintertime storms, Part II: Spatial distribution and microphysical characteristics. *J. Clim. Appl. Meteorol.*, **25**, 489–504.

Rauber, R.M., L.O. Grant, D. Feng, and J.B. Snider, 1986: The characteristics and distribution of cloud water over the mountains of northern Colorado during wintertime storms, Part I: Temporal variations. *J. Clim. Appl. Meteorol.*, **25**, 468–488.

Riley, 1937: Aircraft icing zones on the Oakland-Cheyenne airway. *Mon. Weather Rev.*, **65**, 104–108.

Sand, W.R., W.A. Cooper, M.K. Politovich, and D.L. Veal, 1984: Icing conditions encountered by a research aircraft. *J. Clim. Appl. Meteorol.*, **23**, 1427–1440.

Sassen, K., 1986: Supercooled liquid water climatology in winter storms: A preliminary assessment from remote sensing observations. *J. Weather Modif.*, **17**, 30–35.

Snider, J.B., 1988: Radiometric observations of cloud liquid water during FIRE. Proceedings of IGARSS'88, Edinborough, Scotland, 13–16 September, 1988, 261–262.

Snider, J.B., H.M. Burdick, and D.C. Hogg, 1980: Cloud liquid measurements with a ground-based microwave instrument. *Radio Sci.*, **15**, 683–693.

Snider, J.B., T. Uttal, and R.A. Kropfli, 1986: Remote sensor observations of winter orographic storms in southwestern Utah. NOAA Tech. Memo. ERL WPL–139, NOAA Wave Propagation Laboratory, Boulder, CO, 99 pp.

Tucker, W.B., III, 1983: Current procedures for forecasting aviation icing: A review (Special Report). Report CRREL-SR–83–24, Cold Regions Research and Engineering Laboratory, 36 pp.

Uttal, T., J.B. Snider, R.A. Kropfli, and B.W. Orr, 1989: A remote sensing method of measuring atmospheric vapor fluxes: Application to winter mountain storms. *J. Appl. Meteorol.* (Accepted for publication).

Vogel, G.N., 1988: Icing considerations for HALE (High Altitude, Long Endurance) aircraft. Technical Report TR 88–11, Naval Environmental Prediction Research Facility, Monterey, CA, 51 pp.